Four-wave mixing theory for two-photon generation of excitons in thin films of Cu_2O

I. V. Beloussov,[1,*] J. B. Ketterson,[2,†] and Y. Sun[2]

[1]*Institute of Applied Physics, Academy of Sciences of Moldova, 5 Academy str., Kishinev MD-2028, Republic of Moldova*

[2]*Department of Physics and Astronomy, Northwestern University, Evanston, Illinois 60208, USA*

(Received 31 December 2009; revised manuscript received 3 May 2010; published 19 May 2010)

We propose and theoretically investigate a two-photon four-wave mixing experiment to probe for Bose-Einstein condensation of excitons in Cu_2O thin films. A relatively simple set of equations describing the dynamics of the system is obtained for a particular configuration of the three incident beams, and numerical and approximate analytical solutions are found. When one takes into account the boundary conditions, which result in reflections from the interfaces, the characteristics of the resulting phase-conjugated signal will exhibit Fabry-Perot-type oscillations. For film thicknesses equal to a multiple of a half wavelength in the film the resulting signal is enhanced by more than an order of magnitude relative thicknesses that are an odd multiple of a quarter wavelength. In this case the contribution from accompanying excitonic condensates with wave vectors $\pm 2\mathbf{k}$ is minimal. Therefore, the resulting phase-conjugated signal vs the delay time between the pump and probe pulses yields a direct measure of the time evolution only of the exciton condensate with wave vector $\mathbf{k}=\mathbf{0}$.

DOI: 10.1103/PhysRevB.81.205208 PACS number(s): 71.35.−y, 42.50.Md, 42.65.Sf

I. INTRODUCTION

Cuprous oxide has long been considered as a possible candidate for Bose-Einstein condensation (BEC) due to the relatively small mass and long lifetime of excitons in this material.[1–4] The lowest excited states are classified according to the cubic symmetry of the lattice. The 1*s* exciton level is split by the electron-hole exchange interaction into triply degenerate ${}^3\Gamma_{25}^+$ orthoexciton states, with a binding energy $E_b=150$ meV, and a singlet ${}^1\Gamma_2^+$ paraexciton state, with a binding energy $E_b=162$ meV. Due to their even parity, the orthoexcitons states are only quadrupole active while the paraexcitons are optically inactive in one photon-absorption experiments; the latter can be populated from the orthoexciton states by emitting optical phonons. For high-purity samples the lifetime of the orthoexcitons is a few nanoseconds and mainly determined by the rate of conversion to paraexcitons; for paraexcitons the lifetimes are much longer, a few microseconds. BEC of paraexcitons was reported by Lin and Wolfe[5] but the interpretation remains uncertain. BEC of the orthoexcitonic system has not been reported, possibly due to orthopara conversion or exciton-exciton driven recombination restricting the achievable densities.[6]

Most experimental investigations have involved one-photon absorption.[7–10] Electron-hole pairs generated by this process relax toward the 1*s* state of the lowest excitonic series. One decay mode of the 1*s* orthoexcitons involves the creation of optical phonons. The relaxation of optically generated electron-hole pairs results in a temperature rise of the exciton gas and the density of the orthoexcitons always saturates below the critical density for BEC. Hence, BEC of the orthoexcitons has not been realized by the one-photon excitation.

Several studies on resonant two-photon excitation of 1*s* excitons at low temperatures have been reported.[11–16] The interest was driven by the possibility of directly producing a cooler high-density gas of nearly zero-momentum orthoexcitons.

We recently suggested[17,18] using a two-photon process to directly generate and then probe excitons in a 1*s* state with wave vector $\mathbf{k}=\mathbf{0}$. To perform such experiments, one divides the incoming laser pulse into three beams, 1, 2, and 3. Two of the beams (1 and 3), the pump beams, simultaneously enter the sample from opposite directions. As a result, a macroscopic coherent state of excitons with $\mathbf{k}=\mathbf{0}$ arises that we may think of as a nonequilibrium condensate. Then, under the action of a suitably delayed probe pulse (2) entering the sample at some small angle relative to one of the pump pulses, a phase-conjugated electromagnetic signal (4) arises due to stimulated radiation from the previously generated coherent exciton ensemble, which propagates in direction *opposite* to the probe pulse. The time interval between the probe pulse 2 and pump pulses 1 and 3 can be varied by virtue of an optical delay line. Then, by measuring the intensity of the resulting signal 4, one can monitor the exciton condensate after its creation. Note that a thermal (incoherent) distribution of orthoexcitons does not lead to macroscopic coherent backscattering. Similar methods, generally termed *four-wave mixing*,[19–24] have proved to be powerful tools to investigate coherent excitations in various systems, along with the scattering processes which destroy this coherence (see, e.g., Refs. 25–38).

Our earlier work[18] showed that the total number of photons generated in the course of the experiment was proportional to the areas of all three incoming pulses. The dependence of the resulting time-integrated signal on the delay time t_d is the same as the exciton density dependence on the time t. Hence, one may directly study the time evolution of the exciton condensate. It was also noted that an exciton condensate arising by an alternate route can also be probed through a phase-conjugated two-photon process.

Only the simpler problem involving the time evolution of coherent excitons and photons under the internal electromagnetic fields was considered in our previous study; photon lifetimes were treated phenomenologically by introducing a decay constant γ_{ph} (which is inversely proportional to the photon time of flight through the sample). The reflection/

transmission at the sample boundaries was not taken into account; i.e., the relation between the internal fields and those incidents on the crystal was not obtained and growth of the condensate due to the presence of reflected electromagnetic waves was not taken into account. In particular, how the intensity of the resulting four-wave mixing signal depends on the sample thickness was left as an open question.

In the present paper we discuss four-wave mixing in a crystal of finite thickness, a thin Cu_2O film or platelet; in addition, we will assume that the thickness is considerably less than the spatial extension of laser pulses incident on the film. The pump pulses 1 and 3 are assumed to arrive simultaneously from opposite sides and normal to its surface; the probe pulse makes a small angle with one of the pump pulses.

For the case of a sample with a finite thickness additional phenomena occur: (1) Only part of the amplitude of the incident pulses enters the film; the remaining part being reflected. (2) The parts inside the film undergo multiple reflections which interfere with each other. The excitonic condensate with wave vector $\mathbf{k}=\mathbf{0}$ is generated by those combinations of forward and backward waves having orthogonal polarizations. (3) Primary and reflected waves propagating in the same direction produce additional condensate amplitudes with wave vectors $2\mathbf{k}$ (forward) and $-2\mathbf{k}$ (backward). (4) The additional condensates can act back on the electromagnetic fields that excite them and in this way influence the dynamics of the condensate with wave vector $\mathbf{k}=\mathbf{0}$. (5) For small incident angles Θ, the probe pulse and the resulting four-wave mixing signal also undergo multiple reflections from the film boundaries which interact with the region where the excitons produced by the pump beams reside. In this case the resulting four-wave mixing signal is formed not only by emission from the condensate at $\mathbf{k}=\mathbf{0}$ but also by emission from an additional condensates with wave vectors $\pm 2\mathbf{k}$. Consequently, the resulting four-wave mixing signal involves the dynamics of the excitonic system as a whole; i.e., all components contribute.

The last circumstance calls in question whether the main result of Ref. 18 is valid; i.e., that the study of the dependence of the time-integrated four-wave mixing signal on the delay time between the probe and pump pulses allows monitoring the dynamics of the excitonic condensate with wave vector $\mathbf{k}=\mathbf{0}$.

In the present paper we will show that, for a wide-range experimental conditions, accounting for the finite dimensions of the crystal reduces to incorporating a geometrical factor in the result obtained in Ref. 18. We determine the conditions for which the contribution of the $\pm 2\mathbf{k}$ condensates is minimal and the resulting signal reaches its maximum value. We will also discuss how to experimentally separate the time-integrated resulting signal from the pump and probe pulses generating the condensates.

We start from a set of equations for the macroscopic amplitude of the excitonic density and the electromagnetic field strength supplemented by the Maxwell-Fresnel conditions for the tangential components of electrical and magnetic fields at the film-vacuum boundaries. These equations follow from the model Hamiltonian taking into account the selection rules for two-photon transitions in Cu_2O. We use the same physical assumptions related to the intensity and duration of incoming pulses as in Ref. 18.

This paper is organized as follows. In Sec. II a closed set of nonlinear differential equations is found for the slowly changing macroscopic amplitudes of excitonic and electromagnetic waves inside the film that satisfy the boundary conditions corresponding to a particular configuration of electromagnetic pulses incident on the film. In Sec. III, the set of equations is simplified using some approximations that correspond to the adopted physical assumptions. In Sec. IV we provide the analytical solution of a simplified set of equations and discuss the physical results. Our conclusions are given in Sec. V.

II. BASIC EQUATIONS

We start from the set of macroscopic equations for the positive-frequency components of the electromagnetic field strength $\mathbf{E}^{(+)}(\mathbf{r},t)$ (with polarization $\lambda=1,2$) and exciton amplitudes $\Phi_\alpha^{(+)}(\mathbf{r},t)$ (with $\alpha=xy,yz,zx$)

$$\left(i\hbar\frac{\partial}{\partial t}-\hbar\omega_{ex}(0)+\frac{\hbar^2}{2m_{ex}}\Delta+i\hbar\gamma_{ex}\right)\Phi_{ij}^{(+)}=-GE_i^{(+)}E_j^{(+)}\quad(i,j=x,y,z),$$

$$\left(\Delta-\frac{\varepsilon_b}{c^2}\frac{\partial^2}{\partial t^2}\right)\mathbf{E}^{(+)}=\frac{4\pi}{c^2}\frac{\partial^2}{\partial t^2}\mathbf{P}^{(+)},\tag{1}$$

where

$$P_x^{(+)}=G(E_z^{(-)}\Phi_{zx}^{(+)}+\Phi_{xy}^{(+)}E_y^{(-)}),$$

$$P_y^{(+)}=G(E_x^{(-)}\Phi_{xy}^{(+)}+\Phi_{yz}^{(+)}E_z^{(-)}),$$

$$P_z^{(+)}=G(E_y^{(-)}\Phi_{yz}^{(+)}+\Phi_{zx}^{(+)}E_x^{(-)}),$$

$$E_i^{(-)}=E_i^{(+)*},\quad(i=x,y,z)\tag{2}$$

with $\hbar\omega_{ex}(0)$ and γ_{ex} the energy of formation and the phenomenological decay constant of excitons, m_{ex} the exciton effective mass, ε_b the background dielectric constant of the medium, c the speed of light in vacuum, and G the interaction constant. The set of Eqs. (1) and (2) is analogous to the well-known Keldysh equations[39] for the macroscopic amplitudes of interacting coherent excitons and photons, which can easily be obtained from the Hamiltonian

$$H=H_{ex}+H_{ph}+H_{int},$$

$$H_{ex}=\sum_{\mathbf{k}}\hbar\omega_{ex}(\mathbf{k})\sum_{\alpha=xy,yz,zx}\hat{a}_\alpha^\dagger(\mathbf{k})\hat{a}_\alpha(\mathbf{k}),$$

$$H_{ph}=\sum_{\mathbf{k}}\hbar\omega_{ph}(\mathbf{k})\sum_{\lambda=1,2}\hat{c}_\lambda^\dagger(\mathbf{k})\hat{c}_\lambda(\mathbf{k}),$$

$$H_{int}=\frac{1}{2!\sqrt{V}}\sum_{\mathbf{k}_1,\mathbf{k}_2}\sum_{\alpha=xy,yz,zx}\sum_{\lambda_1,\lambda_2=1,2}g_\alpha^{(\lambda_1,\lambda_2)}(\mathbf{k}_1,\mathbf{k}_2)[\hat{a}_\alpha^\dagger(\mathbf{k}_1+\mathbf{k}_2)\hat{c}_{\lambda_1}(\mathbf{k}_1)\hat{c}_{\lambda_2}(\mathbf{k}_2)+\text{H.c.}],$$

where $\hbar\omega_{ex}(\mathbf{k})=\hbar\omega_{ex}(0)+\hbar^2\mathbf{k}^2/2m_{ex}$ and $\hbar\omega_{ph}(\mathbf{k})$

$=\hbar c|\mathbf{k}|/\sqrt{\varepsilon_b}$ are the energies of the excitons and photons in a state with wave vector $\mathbf{k}$ while $\hat{a}_\alpha^\dagger(\mathbf{k})$ and $\hat{c}_\lambda^\dagger(\mathbf{k})$ are the creation operators of excitons ($\alpha=xy,yz,zx$) and photons ($\lambda=1,2$) with $\hat{a}_\alpha(\mathbf{k})$, $\hat{c}_\lambda(\mathbf{k})$ are corresponding annihilation operators, which collectively satisfy the Bose commutation relationships. The constant $G=(\varepsilon_b/\pi E_g)g$, where E_g is the semiconductor energy gap. The interaction constants $g_\alpha^{(\lambda_1,\lambda_2)}(\mathbf{k}_1,\mathbf{k}_2)$ are proportional to matrix elements of the two-photon transitions calculated in second-order perturbation theory.[40] Using the selection rules for these transitions,[41] we can write these constants in the form

$$g_{xy}^{(\lambda_1,\lambda_2)}(\mathbf{k}_1,\mathbf{k}_2)=e_x^{(\lambda_1)}(\mathbf{k}_1)e_y^{(\lambda_2)}(\mathbf{k}_2)+e_y^{(\lambda_1)}(\mathbf{k}_1)e_x^{(\lambda_2)}(\mathbf{k}_2),$$

$$g_{yz}^{(\lambda_1,\lambda_2)}(\mathbf{k}_1,\mathbf{k}_2)=e_y^{(\lambda_1)}(\mathbf{k}_1)e_z^{(\lambda_2)}(\mathbf{k}_2)+e_z^{(\lambda_1)}(\mathbf{k}_1)e_y^{(\lambda_2)}(\mathbf{k}_2),$$

$$g_{zx}^{(\lambda_1,\lambda_2)}(\mathbf{k}_1,\mathbf{k}_2)=e_z^{(\lambda_1)}(\mathbf{k}_1)e_x^{(\lambda_2)}(\mathbf{k}_2)+e_x^{(\lambda_1)}(\mathbf{k}_1)e_z^{(\lambda_2)}(\mathbf{k}_2),$$

where $\mathbf{e}^{(1)}(\mathbf{k})$ and $\mathbf{e}^{(2)}(\mathbf{k})$ are the two linearly independent polarization vectors of the electromagnetic field with wave vector $\mathbf{k}$; they satisfy the condition $\mathbf{e}^{(1)}(\mathbf{k})\times\mathbf{e}^{(1)}(\mathbf{k})=\mathbf{k}/|\mathbf{k}|$.

We will consider a configuration of incident electromagnetic fields 1, 2, and 3 for which Eqs. (1) and (2) acquire the simplest form.[17] Namely, we choose its wave vectors $\mathbf{k}_1^{(0)}$, $\mathbf{k}_2^{(0)}$, and $\mathbf{k}_3^{(0)}$ to have the form $\mathbf{k}_3^{(0)}=-\mathbf{k}_1^{(0)}=(\omega_0/c)\hat{\mathbf{y}}$, $\mathbf{k}_2^{(0)}=(\omega_0/c)(\hat{\mathbf{x}}\sin\Theta+\hat{\mathbf{y}}\cos\Theta)$, and the polarizations as $\mathbf{e}_1=\mathbf{e}_2=\hat{\mathbf{z}}$, and $\mathbf{e}_3=\hat{\mathbf{x}}$; here $\hat{\mathbf{x}},\hat{\mathbf{y}},\hat{\mathbf{z}}$ the unit vectors defining the Cartesian coordinate system. Then the resulting four-wave mixing electromagnetic signal will have wave vector $\mathbf{k}_4^{(0)}=-\mathbf{k}_2^{(0)}$ and polarization vector $\mathbf{e}_4=\hat{\mathbf{x}}\cos\Theta-\hat{\mathbf{y}}\sin\Theta$. Furthermore we will only discuss the case of very small values of the angle Θ, i.e., $\sin\Theta\ll 1$ and $\cos\Theta\approx 1$. Here $\mathbf{k}_4^{(0)}=-\mathbf{k}_2^{(0)}\approx-(\omega_0/c)\hat{\mathbf{y}}$, $\mathbf{e}_4=\hat{\mathbf{x}}$.

We assume that the pump pulses 1, 3, and the probe pulse 2 are separated by a time interval $t_d\gg t_p$, where t_p is the duration of the pump and probe pulses. In this case, owing to the action of the pump pulses 1 and 3 on the system, only zx excitons are created; exciton creation from the 2,3 or 1,4 combinations is forbidden.

According to the chosen configuration of the incident fields and the aforementioned assumptions, we will search the solution of Eqs. (1) and (2) within the film in the form

$$E_x^{(+)}(\mathbf{r},t)=E_3^{(+)}(y,t)+E_4^{(+)}(y,t),$$

$$E_z^{(+)}(\mathbf{r},t)=E_1^{(+)}(y,t)+E_2^{(+)}(y,t),$$

$$E_{1,4}^{(+)}(y,t)=e^{-i\omega_0 t}[E_{1,4}^{(f)}(y,t)e^{-ik(y-L)}+E_{1,4}^{(b)}(y,t)e^{iky}],$$

$$E_{2,3}^{(+)}(y,t)=e^{-i\omega_0 t}[E_{2,3}^{(f)}(y,t)e^{iky}+E_{2,3}^{(b)}(y,t)e^{-ik(y-L)}],$$

$$\Phi_{zx}^{(+)}(y,t)=e^{-2i\omega_0 t}[\Phi^{(0)}(y,t)e^{ikL}+\Phi^{(f)}(y,t)e^{2iky}+\Phi^{(b)}\times(y,t)e^{-2ik(y-L)}],$$

where $k=\sqrt{\varepsilon_b}\omega_0/c$. Taking into account that the functions 1, e^{iky}, and e^{-iky} are linearly independent and neglecting the nonresonant terms of the form $e^{\pm 3iky}$ on the right-hand side of the second equation in Eq. (1), we obtain the equations for amplitudes $E_i^{(f,b)}(y,t)$ ($i=1,2,3,4$) and $\Phi^{(0,f,b)}(y,t)$, which in the approximation of slowly changing envelopes[42,43] have the following form:

$$\left(\frac{\partial}{\partial t}\pm\frac{c}{\sqrt{\varepsilon_b}}\frac{\partial}{\partial y}\right)\begin{pmatrix}E_1^{(b,f)}(y,t)\\E_4^{(b,f)}(y,t)\end{pmatrix}=\frac{ig}{\hbar}\left[\Phi^{(0)}(y,t)\begin{pmatrix}E_3^{(b,f)*}(y,t)\\E_2^{(b,f)*}(y,t)\end{pmatrix}+\Phi^{(f,b)}(y,t)\begin{pmatrix}E_3^{(f,b)*}(y,t)\\E_2^{(f,b)*}(y,t)\end{pmatrix}\right],$$

$$\left(\frac{\partial}{\partial t}\pm\frac{c}{\sqrt{\varepsilon_b}}\frac{\partial}{\partial y}\right)\begin{pmatrix}E_3^{(f,b)}(y,t)\\E_2^{(f,b)}(y,t)\end{pmatrix}=\frac{ig}{\hbar}\left[\Phi^{(0)}(y,t)\begin{pmatrix}E_1^{(f,b)*}(y,t)\\E_4^{(f,b)*}(y,t)\end{pmatrix}+\Phi^{(f,b)}(y,t)\begin{pmatrix}E_1^{(b,f)*}(y,t)\\E_4^{(b,f)*}(y,t)\end{pmatrix}\right], \tag{3}$$

$$\left\{\frac{\partial}{\partial t}+[\gamma_{ex}+i\Delta(0)]\right\}\Phi^{(0)}(y,t)=\frac{iG}{\hbar}[E_1^{(f)}(y,t)E_3^{(f)}(y,t)+E_2^{(f)}\times(y,t)E_4^{(f)}(y,t)+E_1^{(b)}\times(y,t)E_3^{(b)}(y,t)+E_2^{(b)}\times(y,t)E_4^{(b)}(y,t)],$$

$$\left\{\frac{\partial}{\partial t}+[\gamma_{ex}+i\Delta(2k)]\pm\frac{\hbar k}{m_{ex}}\frac{\partial}{\partial y}\right\}\Phi^{(f,b)}(y,t)=\frac{iG}{\hbar}[E_1^{(b,f)}\times(y,t)E_3^{(f,b)}(y,t)+E_2^{(f,b)}(y,t)E_4^{(b,f)}(y,t)]. \tag{4}$$

where $\Delta(k)=\omega_{ex}(k)-2\omega_0$ is the detuning from the two-photon resonance. As a further simplification of Eqs. (3) and (4) we note that when the film thickness is small we can expand the functions $E_i^{(f,b)}(y,t)$ and $\Phi^{(0,f,b)}(y,t)$ in the variable y, retaining only zeroth-order and first-order terms: $f(y)\approx f(0)+[f(L)-f(0)]y/L$. Again noting that the functions 1 and y are linearly independent, we obtain

$$\frac{\partial}{\partial t}\begin{pmatrix}E_1^{(f)}(0,t)\\E_4^{(f)}(0,t)\end{pmatrix}=-\gamma_{ph}\left[\begin{pmatrix}E_1^{(f)}(0,t)\\E_4^{(f)}(0,t)\end{pmatrix}-\begin{pmatrix}E_1^{(f)}(L,t)\\E_4^{(f)}(L,t)\end{pmatrix}\right]+\frac{ig}{\hbar}\left[\Phi^{(0)}(0,t)\begin{pmatrix}E_3^{(f)*}(0,t)\\E_2^{(f)*}(0,t)\end{pmatrix}+\Phi^{(b)}(0,t)\begin{pmatrix}E_3^{(b)*}(0,t)\\E_2^{(b)*}(0,t)\end{pmatrix}\right],$$

$$\frac{\partial}{\partial t}\begin{pmatrix}E_1^{(b)}(L,t)\\E_4^{(b)}(L,t)\end{pmatrix}=-\gamma_{ph}\left[\begin{pmatrix}E_1^{(b)}(L,t)\\E_4^{(b)}(L,t)\end{pmatrix}-\begin{pmatrix}E_1^{(b)}(0,t)\\E_4^{(b)}(0,t)\end{pmatrix}\right]+\frac{ig}{\hbar}\left[\Phi^{(0)}(L,t)\begin{pmatrix}E_3^{(b)*}(L,t)\\E_2^{(b)*}(L,t)\end{pmatrix}+\Phi^{(f)}(L,t)\begin{pmatrix}E_3^{(f)*}(L,t)\\E_2^{(f)*}(L,t)\end{pmatrix}\right],$$

$$\frac{\partial}{\partial t}\begin{pmatrix} E_3^{(f)}(L,t) \\ E_2^{(f)}(L,t) \end{pmatrix} = -\gamma_{ph}\left[\begin{pmatrix} E_3^{(f)}(L,t) \\ E_2^{(f)}(L,t) \end{pmatrix} - \begin{pmatrix} E_3^{(f)}(0,t) \\ E_2^{(f)}(0,t) \end{pmatrix}\right] + \frac{ig}{\hbar}\left[\Phi^{(0)}(L,t)\begin{pmatrix} E_1^{(f)*}(L,t) \\ E_4^{(f)*}(L,t) \end{pmatrix} + \Phi^{(f)}(L,t)\begin{pmatrix} E_1^{(b)*}(L,t) \\ E_4^{(b)*}(L,t) \end{pmatrix}\right],$$

$$\frac{\partial}{\partial t}\begin{pmatrix} E_3^{(b)}(0,t) \\ E_2^{(b)}(0,t) \end{pmatrix} = -\gamma_{ph}\left[\begin{pmatrix} E_3^{(b)}(0,t) \\ E_2^{(b)}(0,t) \end{pmatrix} - \begin{pmatrix} E_3^{(b)}(L,t) \\ E_2^{(b)}(L,t) \end{pmatrix}\right] + \frac{ig}{\hbar}\left[\Phi^{(0)}(0,t)\begin{pmatrix} E_1^{(b)*}(0,t) \\ E_4^{(b)*}(0,t) \end{pmatrix} + \Phi^{(b)}(0,t)\begin{pmatrix} E_1^{(f)*}(0,t) \\ E_4^{(f)*}(0,t) \end{pmatrix}\right], \tag{5}$$

$$\left\{\frac{\partial}{\partial t} + [\gamma_{ex} + i\Delta(0)]\right\}\Phi^{(0)}(L,t) = \frac{iG}{\hbar}[E_1^{(f)}(L,t)E_3^{(f)}(L,t) + E_2^{(f)}(L,t)E_4^{(f)}(L,t) + E_1^{(b)}(L,t)E_3^{(b)}(L,t) + E_2^{(b)}(L,t)E_4^{(b)}(L,t)],$$

$$\left\{\frac{\partial}{\partial t} + [\gamma_{ex} + i\Delta(0)]\right\}\Phi^{(0)}(0,t) = \frac{iG}{\hbar}[E_1^{(f)}(0,t)E_3^{(f)}(0,t) + E_2^{(f)}(0,t)E_4^{(f)}(0,t) + E_1^{(b)}(0,t)E_3^{(b)}(0,t) + E_2^{(b)}(0,t)E_4^{(b)}(0,t)],$$

$$\left\{\frac{\partial}{\partial t} + [\gamma_{ex} + i\Delta(2k)]\right\}\Phi^{(f)}(L,t) = \frac{iG}{\hbar}[E_1^{(b)}(L,t)E_3^{(f)}(L,t) + E_2^{(f)}(L,t)E_4^{(b)}(L,t)],$$

$$\left\{\frac{\partial}{\partial t} + [\gamma_{ex} + i\Delta(2k)]\right\}\Phi^{(b)}(0,t) = \frac{iG}{\hbar}[E_1^{(f)}(0,t)E_3^{(b)}(0,t) + E_2^{(b)}(0,t)E_4^{(f)}(0,t)]. \tag{6}$$

Here γ_{ph} is the inverse flight time of the photon through the film, $\gamma_{ph}=t_f^{-1}$ and $t_f=\sqrt{\varepsilon_b}L/c$. In the last two of Eqs. (6) we have omitted the terms $\pm\frac{\hbar k}{m_{ex}L}[\Phi^{(f,b)}(L,t) - \Phi^{(f,b)}(0,t)]$, which can be transformed to the form $\pm\gamma_{ph}\varepsilon_b(\hbar\omega_0/m_{ex}c^2)[\Phi^{(f,b)}(L,t) - \Phi^{(f,b)}(0,t)]$. Since the ratio $\hbar\omega_0/m_{ex}c^2$ is small, we can neglect these terms, even for very thin films.

In addition to Eqs. (5) and (6) we have the Maxwell-Fresnel boundary conditions for the tangential components of electric and magnetic fields at the film-vacuum boundary. Assuming that outside the film

$$E_x^{(+)}(\mathbf{r},t) = E_{3,in}^{(+)}(y,t) + E_{3,r}^{(+)}(y,t) + E_{4-w}^{(+)}(y,t), \quad E_z^{(+)}(\mathbf{r},t) = E_{1,t}^{(+)} \times (y,t) + E_{2,in}^{(+)}(y,t) + E_{2,r}^{(+)}(y,t),$$

$$E_{3,in}^{(+)}(y,t) = e^{-i\omega_0 t + ik_0 y}E_3^{(in)}(y,t),$$

$$E_{3,r}^{(+)}(y,t) = e^{-i\omega_0 t - ik_0 y}E_{3,r}(y,t),$$

$$E_{4-w}^{(+)}(y,t) = e^{-i\omega_0 t - ik_0 y}E_{4-w}(y,t),$$

$$E_{1,t}^{(+)}(y,t) = e^{-i\omega_0 t + ik_0 y}E_{1,t}(y,t),$$

$$E_{2,in}^{(+)}(y,t) = e^{-i\omega_0 t + ik_0 y}E_2^{(in)}(y,t),$$

$$E_{2,r}^{(+)}(y,t) = e^{-i\omega_0 t - ik_0 y}E_{2,r}(y,t),$$

for $y \le 0$ and

$$E_x^{(+)}(\mathbf{r},t) = E_{3,t}^{(+)}(y,t) + \tilde{E}_{4-w}^{(+)}(y,t),$$

$$E_z^{(+)}(\mathbf{r},t) = E_{1,in}^{(+)}(y,t) + E_{1,r}^{(+)}(y,t) + E_{2,t}^{(+)}(y,t),$$

$$E_{3,t}^{(+)}(y,t) = e^{-i\omega_0 t + ik_0(y-L)}E_{3,t}^{(in)}(y,t),$$

$$\tilde{E}_{4-w}^{(+)}(y,t) = e^{-i\omega_0 t + ik_0(y-L)}\tilde{E}_{4-w}(y,t),$$

$$E_{1,in}^{(+)}(y,t) = e^{-i\omega_0 t - ik_0(y-L)}E_1^{(in)}(y,t),$$

$$E_{1,r}^{(+)}(y,t) = e^{-i\omega_0 t + ik_0(y-L)}E_{1,r}(y,t),$$

$$E_{2,t}^{(+)}(y,t) = e^{-i\omega_0 t + ik_0(y-L)}E_{2,t}(y,t),$$

for $y \ge L$, we obtain

$$E_1^{(f)}(L,t) = \rho E_1^{(b)}(L,t) + \tau E_1^{(in)}(L,t),$$

$$E_1^{(b)}(0,t) = \rho E_1^{(f)}(0,t),$$

$$E_{2,3}^{(f)}(0,t) = \rho E_{2,3}^{(b)}(0,t) + \tau E_{2,3}^{(in)}(0,t),$$

$$E_{2,3}^{(b)}(L,t) = \rho E_{2,3}^{(f)}(L,t),$$

$$E_4^{(f)}(L,t) = \rho E_4^{(b)}(L,t),$$

$$E_4^{(b)}(0,t) = \rho E_4^{(f)}(0,t), \tag{7}$$

$$E_{4-w}^{(f)}(0,t) = \tau' e^{ikL}E_4^{(f)}(0,t), \tag{8}$$

where $k_0=\omega_0/c$ and

$$\rho = \tilde{\rho}e^{ikL}, \quad \tilde{\rho} = \frac{\sqrt{\varepsilon_b}-1}{\sqrt{\varepsilon_b}+1},$$

$$\tau = \frac{2}{\sqrt{\varepsilon_b}+1}, \quad \tau' = \frac{2\sqrt{\varepsilon_b}}{\sqrt{\varepsilon_b}+1}.$$

Substituting Eq. (7) into Eqs. (5) and (6), we find a closed set of nonlinear differential equations given in Appendix as Eqs. (A1)–(A12) for functions $E_{1,4}^{(f)}(0,t)$, $E_{1,4}^{(b)}(L,t)$, $E_{2,3}^{(f)}(L,t)$, and $E_{2,3}^{(b)}(0,t)$, and $\Phi^{(0)}(L,t)$, $\Phi^{(0)}(0,t)$, $\Phi^{(f)}(L,t)$, and $\Phi^{(b)}(0,t)$.

III. THIN FILMS AND THE EXTERNAL-FIELD APPROXIMATIONS

The complete set of nonlinear equations, taking into account the reaction of the excitons on the electromagnetic waves that generate them, can only be solved using numerical methods. Hence, it is desirable to obtain simpler equations, which can be solved analytically, but do not supply as detailed a description of the temporal evolution of the system. This allows a deeper insight into the physics of the processes which occur in the system.

We consider the set of Eqs. (5)–(7) for bell-shaped incident pulses with a maximum at $t=t_0$. We assume that the pulse duration t_p satisfies the following inequalities:

$$\gamma_{ph}^{-1} \ll t_p \ll \gamma_{ex}^{-1} \tag{9}$$

and the time t_0 is chosen so that $0<t_p \ll t_0$. The first inequality implies that the pulse width t_p is much greater than the time of flight $\sqrt{\varepsilon_b}L/c$, in which case the spatial extent of the pulse $ct_p/\sqrt{\varepsilon_b}$ greatly exceeds the sample thickness L. The second inequality in Eq. (9) facilitates probing the exciton condensate as a function of time and in this way monitoring its temporal evolution.

Taking into account the first of inequalities in Eq. (9), we can neglect the derivatives of the functions $E_{1,4}^{(f)}(0,t)$, $E_{1,4}^{(b)}(L,t)$, $E_{2,3}^{(f)}(L,t)$, and $E_{2,3}^{(b)}(0,t)$ on the left-hand sides of Eqs. (A1)–(A8). As a result, we obtain algebraic equations that allow us to express $E_{1,4}^{(f)}(0,t)$, $E_{1,4}^{(b)}(L,t)$, $E_{2,3}^{(f)}(L,t)$, and $E_{2,3}^{(b)}(0,t)$ via the amplitudes $\Phi^{(0)}(L,t)$, $\Phi^{(0)}(0,t)$, $\Phi^{(f)}(L,t)$, and $\Phi^{(b)}(0,t)$. Substituting the resulting expressions into Eqs. (A9)–(A12), we find equations that define the temporal evolution of excitonic condensates.

The procedure can be further simplified by suppressing the reaction of generated excitons on the incident laser pulses. In this case the amplitudes $E_i^{(f,b)}$ $(i=1,2,3,4)$ will depend only on the background dielectric constant of the film ε_b and on its thickness L. In fact, if we omit the time derivatives in Eqs. (A1)–(A8) and neglect the second of the terms on the right-hand side, we find $E_i^{(f,b)}(L,t)=E_i^{(f,b)}(0,t)$ $(i=1,2,3,4)$. Assuming $E_1^{(in)}(L,t)=E_{2,3}^{(in)}(0,t)=E^{(in)}(t)$ $=E^{(in)}(t_0)f(t)$, we obtain that in the zero-order approximation the known result[44]

$$E_i^{(f,b)}(L,t) = \tau E^{(in)}(t_0) F_i^{(f,b)}(L,t), \tag{10}$$

where $i=1,2,3,4$

$$F_1^{(b)}(L,t) = F_3^{(b)}(0,t) = \frac{\rho f(t)}{1-\rho^2},$$

$$F_1^{(f)}(0,t) = F_3^{(f)}(L,t) = \frac{f(t)}{1-\rho^2},$$

$$F_2^{(b)}(0,t) = \frac{\rho f(t-t_d)}{1-\rho^2},$$

$$F_2^{(f)}(L,t) = \frac{f(t-t_d)}{1-\rho^2},$$

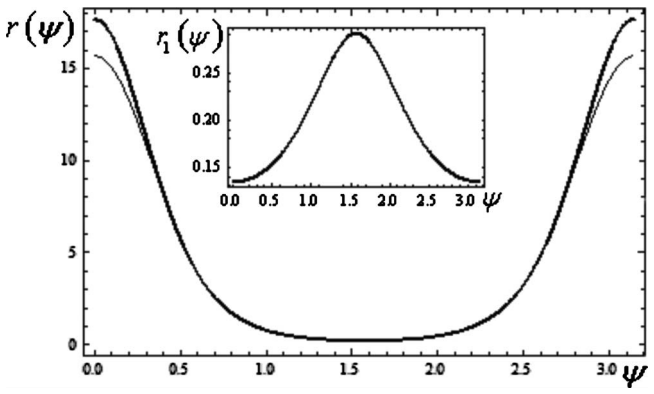

FIG. 1. The thick curve describes the dependence $r(\psi)$ in the interval $(0,\pi)$ while the thin curve describes its expansion in a series in the parameter $\tilde{\rho}$ with the accuracy to terms of the order of $\tilde{\rho}^6$. The curve in the inset describes the dependence $r_1(\psi)$ in the interval $(0,\pi)$.

$$F_4^{(f,b)}(L,t) = F_4^{(f,b)}(0,t) = 0. \tag{11}$$

Substituting Eqs. (10) and (11) into Eqs. (A1)–(A8) and assuming that $\Delta(2k)\approx\Delta(0)$, since the ratio $\hbar\omega_0/m_{ex}c^2$ is small, we obtain

$$\Phi^{(0)}(L,t) = \Phi^{(0)}(0,t) = \frac{\tau\rho}{(1-\rho^2)^2}\Phi(t)\sqrt{\frac{\varepsilon_b E^{(in)2}(t_0)/2\pi}{\hbar\omega_0}},$$

$$\Phi^{(f)}(L,t) = \Phi^{(b)}(0,t) = \frac{\tau(1+\rho^2)}{(1-\rho^2)^2}\Phi(t)\sqrt{\frac{\varepsilon_b E^{(in)2}(t_0)/2\pi}{\hbar\omega_0}}, \tag{12}$$

where function $\Phi(t)$ satisfies the equation

$$\left[\frac{\partial}{\partial\bar{t}} + (1+i\bar{\Delta})\right]\Phi(\bar{t}) = i\xi f^2(\bar{t}), \tag{13}$$

where

$$\bar{t} = \gamma_{ex}t, \quad \bar{\Delta} = \Delta(0)/\gamma_{ex},$$

$$\xi = \frac{g}{\hbar\gamma_{ex}}\sqrt{\frac{\varepsilon_b E^{(in)2}(t_0)/2\pi}{\hbar\omega_0}}.$$

IV. DISCUSSION AND MAIN RESULTS

The approximate solution of Eq. (13) for the resonant case $t_p\Delta(0)\ll 1$ and Gaussian incident pulses with a maximum $t=t_0$ $(t_p \ll t_0)$

$$f(\bar{t}) = \exp\left[-2\frac{(\bar{t}-\bar{t}_0)^2}{\bar{t}_p^2}\right]$$

was obtained in Ref. 18 in the form

$$\Phi(\bar{t}) \approx -i\xi\sigma(\bar{t})\exp[-(1+i\bar{\Delta})(\bar{t}-\bar{t}_0)],$$

where

$$\sigma(\bar{t}) = \frac{\sqrt{\pi}\bar{t}_p}{4}\left\{\mathrm{erf}\left(2\frac{\bar{t}_0}{\bar{t}_p}\right) + \mathrm{erf}\left[2\frac{(\bar{t}-\bar{t}_0)}{\bar{t}_p}\right]\right\} \approx \frac{\sqrt{\pi}\bar{t}_p}{4}\left\{1 + \mathrm{erf}\left[2\frac{(\bar{t}-\bar{t}_0)}{\bar{t}_p}\right]\right\}.$$

We now account for the stimulated radiation, and the resulting four-wave mixing signal 4, arising from the pump pulses 1, 3 and the probe pulse 2. Substituting Eq. (12) into Eqs. (A7) and (A8), and neglecting the time derivatives, we obtain

$$\begin{cases} F_4^{(f)}(0,\bar{t}) - \rho F_4^{(b)}(L,\bar{t}) = \dfrac{i\xi}{\bar{\gamma}_{ph}}\dfrac{1+|\rho|^2+\rho^2}{(1-\rho^2)^2(1-\rho^{*2})}\Phi(\bar{t})f(\bar{t}-\bar{t}_d) \\ -\rho F_4^{(f)}(0,\bar{t}) + F_4^{(b)}(L,\bar{t}) = \dfrac{i\xi}{\bar{\gamma}_{ph}}\dfrac{\rho^*(1+\rho^2+\rho^2/|\rho|^2)}{(1-\rho^2)^2(1-\rho^{*2})}\Phi(\bar{t})f(\bar{t}-\bar{t}_d), \end{cases} \tag{14}$$

where $\bar{\gamma}_{ph}=\gamma_{ph}/\gamma_{ex}$.

It follows from Eq. (14) that

$$F_4^{(f)}(0,\bar{t}) = \frac{i\xi}{\bar{\gamma}_{ph}}\frac{(1+2|\rho|^2)+\rho^2(2+|\rho|^2)}{(1-\rho^2)^2|1-\rho^2|^2}\Phi(\bar{t})f(\bar{t}-\bar{t}_d)$$

and using the second of inequalities in Eq. (9)

$$F_4^{(f)}(0,\bar{t}) \approx \frac{i\xi}{\bar{\gamma}_{ph}}\frac{(1+2|\rho|^2)+\rho^2(2+|\rho|^2)}{(1-\rho^2)^2|1-\rho^2|^2}\Phi(\bar{t}_0+\bar{t}_d)f(\bar{t}-\bar{t}_d).$$

Taking into account Eq. (8), we find that the flux density of the resulting four-wave mixing signal $S_{4-w}(t) = cE_{4-w}^2(0,t)/2\pi$ is proportional to the flux density of the probe pulse $S_{in}(t)=cE^{(in)2}(t_0)/2\pi$

$$S_{4-w}(t) = (\tau\tau')^2 r(kL)\frac{\xi^2}{\bar{\gamma}_{ph}^2}|\Phi(t_0+t_d)|^2 S_{in}(t), \tag{15}$$

where

$$r(kL) = \frac{(1+\tilde{\rho}^2)^2}{(1-\tilde{\rho}^2)^6}\frac{1+\dfrac{(1+2\tilde{\rho}^2)(2+\tilde{\rho}^2)}{(1+\tilde{\rho}^2)^2}\left(\dfrac{2\tilde{\rho}}{1-\tilde{\rho}^2}\right)^2\cos^2 kL}{\left[1+\left(\dfrac{2\tilde{\rho}}{1-\tilde{\rho}^2}\right)^2\sin^2 kL\right]^4}. \tag{16}$$

The factor $(\tau\tau')^2$ in Eq. (15) appears since the strength of the electric component of the incident probe pulse 2 changes its value at the crystal interface from $E^{(in)}$ to $\tau E^{(in)}$; and vice versa, the strength of the electric component of the resulting electromagnetic signal 4 leaving the crystal changes its value from E_{4-w} to $\tau' E_{4-w}$. For Cu_2O we have $(\tau\tau')^2 \approx 0.655$. The "geometrical factor" $r(kL)$ takes into account the multiple internal reflections of pulses 1–4 from the crystal/vacuum interfaces. Assuming $\tilde{E}^{(in)}(t)=\tau E^{(in)}(0,t)$ and $E_{4-w}(0,t) = \tau'\tilde{E}_{4-w}(t)$ in Eq. (15), we find for $\tilde{\rho}=0$ $[r(kL)\equiv 1]$ that

$$S_{4-w}(t) = \frac{\xi^2}{\bar{\gamma}_{ph}^2}|\Phi(t_0+t_d)|^2\tilde{S}(t),$$

where $\tilde{S}(t)=(c/\sqrt{\varepsilon_b})[\varepsilon_b\tilde{E}^2(t)/2\pi]$ is the flux density inside the crystal; i.e., we come to the result of Ref. 18, where only the interaction of excitons with the direct waves inside the crystal was studied. Our description allows one to associate these waves with the waves outside the crystal, the incident waves 1–3 and outgoing wave 4.

According to Eq. (15), $S_{4-w}\propto L^2 r(kL)$. The function $r(\psi)$ is periodic with period π. Figure 1 shows this function in the interval $(0,\pi)$. As can be seen from the figure, the intensity of the resulting signal depends significantly on the film thickness; for $L=(\lambda/2)n$ $(n=1,2,3,\ldots)$ it exceeds the intensity predicted in Ref. 18 by a factor of 17.7 while for $L=(\lambda/4)n$ it is smaller by a factor of 4.5, where $\lambda = 2\pi c/\omega_0\sqrt{\varepsilon_b}$ is the wavelength of laser radiation in the film. In particular, the condition $L=(\lambda/2)$ is satisfied for a film with a thickness of $L=2.391\times 10^{-5}$ cm.

Thus, for $L=(\lambda/2)n$ $(n=1,2,3,\ldots)$ the resulting signal is larger than the case when $L=(\lambda/4)n$ $(n=1,3,5,\ldots)$, by a factor of 77 for Cu_2O.[45] This is easily understood since $L=(\lambda/2)n$ $(n=1,2,3,\ldots)$ is the condition for maximum transmission through the Fabry-Perot cavity formed by reflection from the interfaces, which simultaneously involves the largest amplitude inside the crystal. Obviously, the larger parts of the incident pulses enter inside the film, the larger quantity of excitons are generated in it; therefore, the larger value of the resulting signal should be expected. However, note that the resulting signal is not a simple multiplication of the intensities of the incident pulses [see Eqs. (15) and (16)].

The time evolution of the excitonic condensate with wave vector $\mathbf{k}=\mathbf{0}$ is of primary interest. The ratio

$$\frac{|\Phi^{(f,b)}|^2}{|\Phi^{(0)}|^2} = r_1(kL) \tag{17}$$

of the number of excitons with wave vector $\pm 2\mathbf{k}$ to the number of excitons with wave vector $\mathbf{k}=\mathbf{0}$ is defined by the relationship

$$r_1(kL) = \frac{1}{4}\frac{\left(\dfrac{2\tilde{\rho}}{1-\tilde{\rho}^2}\right)^2}{1+\left(\dfrac{2\tilde{\rho}}{1-\tilde{\rho}^2}\right)^2\cos^2 kL}$$

and it is a periodic function of the variable kL with the period π. This function in the interval $(0,\pi)$ is shown in the inset of Fig. 1. As can be seen in the figure, the ratio in Eq. (17) is minimal and amounts to 0.13 for $L=(\lambda/2)n$ $(n=1,2,3,\ldots)$, i.e., for those film thicknesses for which the resulting elec-

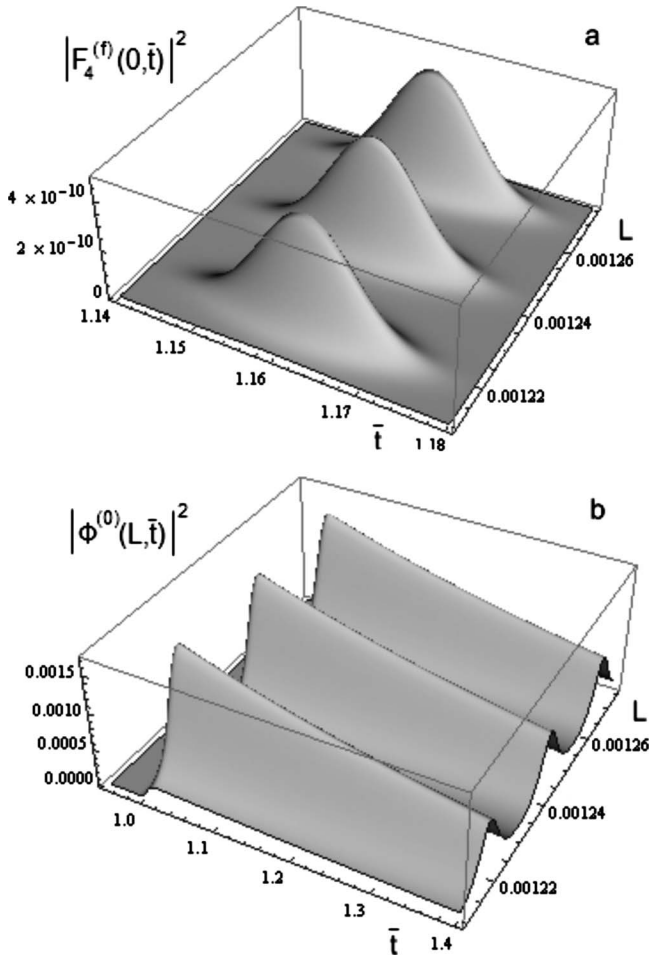

FIG. 2. Dependencies of (a) $|F_4^{(f)}(0,\bar{t})|^2$ and (b) $|\Phi^{(0)}(L,\bar{t})|^2$ versus $\bar{t}$ and L for $\varepsilon_b=6.5$, $\hbar\gamma_{ex}=1$ μeV, $\bar{t}_p=0.016$, $\bar{t}_d=0.16$, $\bar{t}_0=1$, and for the flux density of pulses incident on the crystal $S=1$ MW/cm^2.

tromagnetic signal 4 attains its maximal value. This nontrivial result tells us that the four-wave mixing signal is a direct measure of the temporal dynamics of the condensate with wave vector $\mathbf{k}=\mathbf{0}$, which is of primary interest for us.

From Fig. 2 we see that the maximal values of the flux density of the resulting signal occurs at the same film thicknesses $L=(\lambda/2)n$ for which the exciton density is maximal. In particular, the maxima in Fig. 2 correspond to the values $n=51,52,53$. Both the exciton density and the phase conjugated signal 4 increase when L increases.

The numerical solution of the complete set of nonlinear differential Eqs. (A1)–(A12) for the functions $E_{1,4}^{(f)}(0,t)$, $E_{1,4}^{(b)}(L,t)$, $E_{2,3}^{(f)}(L,t)$, and $E_{2,3}^{(b)}(0,t)$, and $\Phi^{(0)}(L,t)$, $\Phi^{(\bar{0})}(0,t)$, $\Phi^{(f)}(L,t)$, and $\Phi^{(b)}(0,t)$ in the presence of an incident flux $S=(1/100)$ MW/cm^2 leads to results that accurately coincide with the analytical results obtained above by virtue of various approximations.

We note that real laser beams have a (typically Gaussian) spatial distribution of the electromagnetic field intensity in the plane perpendicular to the propagation direction. As an approximation we will assume that the pump beams (1 and 3) generate excitons in a cylinder with its diameter d and height L inside the film. The probe (2) and resulting (4) beams can leave this region after they have undergone only a finite number of reflections $N\sim d/2L\tan\Theta$ from the internal crystal boundaries. In the absence multiple reflections of the probe 2 and resulting 4 beams inside the active, exciton-filled, region, the geometrical factor is given by

$$r'(kL)=\frac{1}{(1-\tilde{\rho}^2)^2}\frac{1+\left(\frac{2\tilde{\rho}}{1-\tilde{\rho}^2}\right)^2\cos^2 kL}{\left[1+\left(\frac{2\tilde{\rho}}{1-\tilde{\rho}^2}\right)^2\sin^2 kL\right]^2},$$

which results in only a tenfold enhancement of the resulting signal for $L=(\lambda/2)n$ $(n=1,2,3,\ldots)$ in comparison with the case when $L=(\lambda/4)n$ $(n=1,3,5,\ldots)$. Equation (16) was obtained with the assumption that the beams 2 and 4 undergo an infinite number of reflections. If we expand the expression (16) in a series in the parameter $\tilde{\rho}$ then each term of the expansion corresponds to one reflection from the internal boundaries. It is easy to show that it is sufficient to take into account only the first six terms of the series to obtain a result close to the exact Eq. (16) (see Fig. 1). Hence, the Eq. (16) also remains valid for a finite transverse distribution of the beams when $N>6$.

The smaller the film thickness and the angle of incidence of the probe beam, the larger is the number of reflections of the beam from the film boundaries and with it the resulting signal. However, for small angles Θ, or for the limiting case of a normal incidence of the probe pulse 2 $(\Theta=0)$, the four-wave mixing signal 4 copropagates with transmitted or reflected pulses arising from pulses 1, 2, and 3. However pump pulses 1 and 3 precede the probe pulse 2, and since $t_d\gg t_p$ the resulting signal 4 and the part of the pulse 2 reflected from the film surface are *cross polarized* and therefore can be separated using a polarizer.

On the other hand, the resulting four-wave mixing signal is weak since the interaction constant for the two-photon generation of excitons is small so it may be difficult to observe experimentally. But one can also study the time-integrated signal, the value of which can be increased as a result of multiple repetitions of the experiment over time intervals spaced by a time $t\gg 1/\gamma_{ex}$. According to Ref. 18, the dependence of the time-integrated signal on the delay time t_d for $t_d\gg t_p$ follows the dependence of the exciton condensate density on the time t. While studying the time-integrated signal for extremely small angles Θ, it is quite difficult to select the emissions from various pulses using a finite delay time between the pump and probe pulses. However, note that the polarization and direction of propagation of the resulting signal coincide with those only for the part of the pump pulse 3 reflected from the film. For the optimal experimental conditions, when $L=(\lambda/2)n$ $(n=1,2,3,\ldots)$, a complete transmission of the three incident pulses 1, 2, and 3 occurs; this means, that all three pulses pass through the film without reflection. Therefore, in this case only the resulting signal 4 and the pump pulse 1 passed through the film without reflection will propagate in the direction $-\hat{\mathbf{y}}$ to the left from the film (for $y<0$). These pulses are cross polarized and it is easy to separate them.

V. CONCLUSIONS

In the presence of crystal boundaries, four-wave mixing results in the four direct electromagnetic waves, a train of reflected waves, and additional waves of excitonic polarization. Owing to the interference of these waves and their interaction, a nonmonotonic dependence of the resulting four-wave mixing signal on the film thickness occurs. Thicknesses that are a multiple of a half wavelength of the laser radiation in the film, implying a spatial resonance, produce the largest response. The presence of a complex wave interference does not change the central result of Ref. 18: the dependence of the resulting time-integrated electromagnetic signal as a function of the time delay between the pump and the probe pulses exhibits the same behavior as the exciton condensate density.

ACKNOWLEDGMENTS

We are grateful to S. A. Moskalenko and P. I. Khadzhi for fruitful discussions. At Northwestern the work was supported by NSF under Grant No. 0353831.

APPENDIX: FULL SET OF EQUATIONS FOR THE MACROSCOPIC AMPLITUDES OF ELECTROMAGNETIC AND EXCITONIC WAVES

After the approximation of slowly changing envelopes and the thin-film approximation were used the basic set of equations has the following form:

$$\frac{\partial}{\partial t}E_3^{(f)}(L,t) = -\gamma_{ph}[E_3^{(f)}(L,t) - \rho E_3^{(b)}(0,t) - \tau E_3^{(in)}(0,t)] + \frac{ig}{\hbar}\{\Phi^{(0)}(L,t)[\rho E_1^{(b)}(L,t) + \tau E_1^{(in)}(L,t)]^* + \Phi^{(f)} \times (L,t)E_1^{(b)*}(L,t)\}, \tag{A1}$$

$$\frac{\partial}{\partial t}E_3^{(b)}(0,t) = -\gamma_{ph}[E_3^{(b)}(0,t) - \rho E_3^{(f)}(L,t)] + \frac{ig}{\hbar}\{\Phi^{(0)}(0,t)[\rho E_1^{(f)} \times (0,t)]^* + \Phi^{(b)}(0,t)E_1^{(f)*}(0,t)\}, \tag{A2}$$

$$\frac{\partial}{\partial t}E_1^{(b)}(L,t) = -\gamma_{ph}[E_1^{(b)}(L,t) - \rho E_1^{(f)}(0,t)] + \frac{ig}{\hbar}\{\Phi^{(0)}(L,t)[\rho E_3^{(f)} \times (L,t)]^* + \Phi^{(f)}(L,t)E_3^{(f)*}(L,t)\}, \tag{A3}$$

$$\frac{\partial}{\partial t}E_1^{(f)}(0,t) = -\gamma_{ph}[E_1^{(f)}(0,t) - \rho E_1^{(b)}(L,t) - \tau E_1^{(in)}(L,t)] + \frac{ig}{\hbar}\{\Phi^{(0)}(0,t)[\rho E_3^{(b)}(0,t) + \tau E_3^{(in)}(0,t)]^* + \Phi^{(b)} \times (0,t)E_3^{(b)*}(0,t)\}, \tag{A4}$$

$$\frac{\partial}{\partial t}E_2^{(f)}(L,t) = -\gamma_{ph}[E_2^{(f)}(L,t) - \rho E_2^{(b)}(0,t) - \tau E_2^{(in)}(0,t-t_d)] + \frac{ig}{\hbar}\{\Phi^{(0)}(L,t)[\rho E_4^{(b)}(L,t)]^* + \Phi^{(f)} \times (L,t)E_4^{(b)*}(L,t)\}, \tag{A5}$$

$$\frac{\partial}{\partial t}E_2^{(b)}(0,t) = -\gamma_{ph}[E_2^{(b)}(0,t) - \rho E_2^{(f)}(L,t)] + \frac{ig}{\hbar}\{\Phi^{(0)}(0,t)[\rho E_4^{(f)} \times (0,t)]^* + \Phi^{(b)}(0,t)E_4^{(f)*}(0,t)\}, \tag{A6}$$

$$\frac{\partial}{\partial t}E_4^{(b)}(L,t) = -\gamma_{ph}[E_4^{(b)}(L,t) - \rho E_4^{(f)}(0,t)] + \frac{ig}{\hbar}\{\Phi^{(0)}(L,t)[\rho E_2^{(f)} \times (L,t)]^* + \Phi^{(f)}(L,t)E_2^{(f)*}(L,t)\}, \tag{A7}$$

$$\frac{\partial}{\partial t}E_4^{(f)}(0,t) = -\gamma_{ph}[E_4^{(f)}(0,t) - \rho E_4^{(b)}(L,t)] + \frac{ig}{\hbar}\{\Phi^{(0)}(0,t)[\rho E_2^{(b)} \times (0,t) + \tau E_2^{(in)}(0,t-t_d)]^* + \Phi^{(b)}(0,t)E_2^{(b)*}(0,t)\}, \tag{A8}$$

$$\left\{\frac{\partial}{\partial t} + [\gamma_{ex} + i\Delta(2k)]\right\}\Phi^{(f)}(L,t) = \frac{iG}{\hbar}[E_1^{(b)}(L,t)E_3^{(f)}(L,t) + E_2^{(f)} \times (L,t)E_4^{(b)}(L,t)], \tag{A9}$$

$$\left\{\frac{\partial}{\partial t} + [\gamma_{ex} + i\Delta(2k)]\right\}\Phi^{(b)}(0,t) = \frac{iG}{\hbar}[E_1^{(f)}(0,t)E_3^{(b)}(0,t) + E_2^{(b)} \times (0,t)E_4^{(f)}(0,t)], \tag{A10}$$

$$\left\{\frac{\partial}{\partial t} + [\gamma_{ex} + i\Delta(0)]\right\}\Phi^{(0)}(L,t) = \frac{iG}{\hbar}\{[\rho E_1^{(b)}(L,t) + \tau E_1^{(in)} \times (L,t)]E_3^{(f)}(L,t) + E_1^{(b)}(L,t) \times [\rho E_3^{(f)}(L,t)] + E_2^{(f)}(L,t) \times [\rho E_4^{(b)}(L,t)] + [\rho E_2^{(f)} \times (L,t)]E_4^{(b)}(L,t)\}, \tag{A11}$$

$$\left\{\frac{\partial}{\partial t} + [\gamma_{ex} + i\Delta(0)]\right\}\Phi^{(0)}(0,t) = \frac{iG}{\hbar}\{E_1^{(f)}(0,t)[\rho E_3^{(b)}(0,t) + \tau E_3^{(in)}(0,t)] + [\rho E_1^{(f)} \times (0,t)]E_3^{(b)}(0,t) + [\rho E_2^{(b)} \times (0,t) + \tau E_2^{(in)}(0,t-t_d)]E_4^{(f)} \times (0,t) + E_2^{(b)}(0,t)[\rho E_4^{(f)} \times (0,t)]\}. \tag{A12}$$

*igor.beloussov@phys.asm.md
†j-ketterson@northwestern.edu

[1] S. A. Moskalenko and D. W. Snoke, *Bose-Einstein Condensation of Excitons and Biexcitons and Coherent Nonlinear Optics With Excitons* (Cambridge University Press, Cambridge, England, 2000).
[2] D. W. Snoke, A. J. Shields, and M. Cardona, Phys. Rev. B **45**, 11693 (1992).
[3] C. Ell, A. L. Ivanov, and H. Haug, Phys. Rev. B **57**, 9663 (1998).
[4] D. Fröhlich, G. Dasbach, G. B. H. von Hoögersthal, M. Bayer, R. Klieber, D. Suter, and H. Stolz, Solid State Commun. **134**, 139 (2005).
[5] J. L. Lin and J. P. Wolfe, Phys. Rev. Lett. **71**, 1222 (1993).
[6] J. I. Jang and J. P. Wolfe, Phys. Rev. B **72**, 241201(R) (2005).
[7] D. Hulin, A. Mysyrowicz, and C. B. à la Guillaume, Phys. Rev. Lett. **45**, 1970 (1980).
[8] D. Snoke, J. P. Wolfe, and A. Mysyrowicz, Phys. Rev. Lett. **59**, 827 (1987).
[9] A. Mysyrowicz, D. W. Snoke, and J. P. Wolfe, Phys. Status Solidi B **159**, 387 (1990).
[10] D. Snoke, J. P. Wolfe, and A. Mysyrowicz, Phys. Rev. B **41**, 11171 (1990).
[11] M. Y. Shen, S. Koyama, M. Saito, T. Goto, and N. Kuroda, Phys. Rev. B **53**, 13477 (1996).
[12] T. Goto, M. Y. Shen, S. Koyama, and T. Yokouchi, Phys. Rev. B **55**, 7609 (1997).
[13] M. Y. Shen, T. Yokouchi, S. Koyama, and T. Goto, Phys. Rev. B **56**, 13066 (1997).
[14] S. Kono, N. Naka, M. Hasuo, S. Saito, T. Suemoto, and N. Nagasawa, Solid State Commun. **97**, 455 (1996).
[15] N. Naka and N. Nagasawa, Solid State Commun. **110**, 153 (1999).
[16] Y. Sun, G. K. L. Wong, and J. B. Ketterson, Phys. Rev. B **63**, 125323 (2001).
[17] I. Beloussov, J. B. Ketterson, and Y. Sun, Solid State Commun. **134**, 135 (2005).
[18] I. V. Beloussov, J. B. Ketterson, and Y. Sun, Phys. Rev. B **80**, 245213 (2009).
[19] H. J. Eichler, P. Gunther, and D. W. Pohl, *Laser-Induced Dynamical Grating* (Springer-Verlag, Berlin, 1980).
[20] Y. R. Shen, *The Principles of Nonlinear Optics* (Wiley, New York, 1984).
[21] J. Shah, *Ultrafast Spectroscopy of Semiconductors and Semiconductor Nanostructures* (Springer-Verlag, Berlin, 1996).
[22] D. S. Chemla and J. Shah, Nature (London) **411**, 549 (2001).
[23] R. L. Sutherland, *Handbook of Nonlinear Optics* (Marcel Dekker, New York, 2003).
[24] V. M. Axt and T. Kuhn, Rep. Prog. Phys. **67**, 433 (2004).
[25] T. Voss, I. Rückmann, J. Gutowski, V. M. Axt, and T. Kuhn, Phys. Rev. B **73**, 115311 (2006).
[26] A. I. Filin, P. D. Persans, K. Babocsi, M. Schmitt, W. Kiefer, V. D. Kulakovskii, and N. A. Gippius, Phys. Rev. B **73**, 125322 (2006).
[27] D. O. Kundys, J.-P. R. Wells, A. D. Andreev, S. A. Hashemizadeh, T. Wang, P. J. Parbrook, A. M. Fox, D. J. Mowbray, and M. S. Skolnick, Phys. Rev. B **73**, 165309 (2006).
[28] J. A. Davis, J. J. Wathen, V. Blanchet, and R. T. Phillips, Phys. Rev. B **75**, 035317 (2007).
[29] Y. Ogawa and F. Minami, Phys. Rev. B **75**, 073302 (2007).
[30] P. Gilliot, S. Cronenberger, H. R. Soleimani, C. Brimont, O. Crégut, M. Gallart, and B. Hönerlage, Phys. Rev. B **75**, 125209 (2007).
[31] S. G. Carter, Z. Chen, and S. T. Cundiff, Phys. Rev. B **76**, 121303(R) (2007).
[32] L. Yang and S. Mukamel, Phys. Rev. B **77**, 075335 (2008).
[33] J. Kasprzak and W. Langbein, Phys. Rev. B **78**, 041103(R) (2008).
[34] H. Oka and H. Ishihara, Phys. Rev. B **78**, 195314 (2008).
[35] M. Erementchouk, M. N. Leuenberger, and L. J. Sham, Phys. Rev. B **79**, 085307 (2009).
[36] A. Sitek and P. Machnikowski, Phys. Rev. B **80**, 115301 (2009).
[37] J. Renger, R. Quidant, N. van Hulst, S. Palomba, and L. Novotny, Phys. Rev. Lett. **103**, 266802 (2009).
[38] J. Renger, R. Quidant, N. van Hulst, and L. Novotny, Phys. Rev. Lett. **104**, 046803 (2010).
[39] L. V. Keldysh, *Problems of Theoretical Physics Dedicated to the Memory of I. E. Tamm* (Nauka, Moscow, 1972), pp. 433–444 (in Russian).
[40] A. I. Bobrysheva, S. A. Moskalenko, and M. I. Shmigliuk, Sov. Phys. Semicond. **1**, 1224 (1968) [Fiz. Tekh. Poluprovodn. **1**, 1469 (1967) (in Russian)].
[41] M. Inoue and Y. Toyozawa, J. Phys. Soc. Jpn. **20**, 363 (1965).
[42] J. A. Armstrong, N. Bloembergen, J. Ducuing, and P. S. Pershan, Phys. Rev. **127**, 1918 (1962).
[43] J. A. Armstrong, S. S. Jha, and N. S. Shiren, IEEE J. Quantum Electron. **6**, 123 (1970).
[44] M. Born and E. Wolf, *Principles of Optics: Electromagnetic Theory of Propagation, Interference and Diffraction of Light* (Cambridge University Press, Cambridge, United Kingdom, 1999).
[45] By inclining the two pump beams relative to the sample normal one can arrange for the projection of the wave vector to satisfy the multiple half-wave or quarter-wave conditions for other L values. The resulting condensates would then have small in-plane components. A similar statement holds for the probe and the four-wave mixing beams, which, since they come in at an angle, would involve a different multiplicative integer.